A general framework for fracture intersection analysis: algorithms and practical applications

Younes Fadakar Alghalandis[1*], Chaoshui Xu[2] and Peter A. Dowd[3]
younes.fadakar@gmail.com
[1, 2] School of Civil, Environmental and Mining Engineering, The University of Adelaide.
[3] Faculty of Engineering, Computer and Mathematical Sciences, The University of Adelaide.

The modelling and simulation of fracture networks is a critical component of the assessment of hot dry rock (HDR) geothermal resources and of the design and creation of enhanced geothermal systems (EGS). The production of geothermal energy from an EGS depends on fluid pathways through the HDR and thus connectivity of fractures is essential. One way of assessing and modelling fracture connectivity is by intersection analysis. There is a notable lack of research in this area reported in the published literature probably because of the extreme complexity of three-dimensional fractures in HDR especially with respect to their geometrical characteristics i.e., shapes and orientations and spatial inter-relationships in the fracture network.

In this paper we present a framework for three-dimensional intersection analysis of fracture networks. The framework includes several robust algorithms for three-dimensional geometrical operations on various data structure configurations. We present two case studies to demonstrate the framework.

The first case study is a stochastic fracture network model generated by Monte Carlo sampling of marked point processes that incorporate the most significant fracture characteristics: location, orientation and shape. The second case study is a database of real measurements of fracture parameters. The proposed framework demonstrates the potential to accommodate any amount of complexity e.g., complicated intersections in a fracture network such as varying intensity, varying geometry and numbers of fractures. The resulting fracture intersection databases can be used for further applications such as statistical and spatial analysis of intersections and connectivity analysis.

Keywords: HDR, fracture intersection, rock fracture modelling, rock fracture connectivity

Introduction

Geothermal energy is expected to make up a substantial portion of the world renewable energy market. The renewed interest in geothermal energy over the past decade has stimulated research and development in areas including reservoir modelling, flow and heat transfer simulations, new equipment and new operational techniques (see MIT-led 2011).

Effective heat production from an EGS requires a fracture network in the rock mass so the heat can be efficiently transferred by means of a carrier (water or CO_2) when it passes through the system from the injection to the production well. Where there is a lack of fluid conducting natural fractures a stimulation operation is applied to extend the existing fractures or to create new fractures so as to enhance the performance of geothermal system. A non-productive fracture system (i.e., isolated fracture clusters) or an ill-connected fracture network could be improved by the stimulation process. One of the major challenges, however, is to obtain a realistic connectivity model between the wells. Such a model is critical to the assessment of the response of the system when it is subjected to fluid flow. The design process for a geothermal system is also affected considerably by the characteristics of the fracture system. In EGS, the host rock is, in general, crystalline and the only effective way to transfer fluid between the wells is through fractures. In other words, the production of geothermal energy from an EGS essentially depends on fluid pathways which are fractures and thus connectivity of fractures is a key factor. The connectivity of fractures in a fracture network is controlled by intersections between fractures and also between fractures and injection and production wells.

Due to the significant depth of the EGS (up to 5km below the surface) and the fact that only a few wells are drilled in an area of a few square kilometres, the direct observation and measurement of fractures is very limited if it not impossible. Thus, in practice, the whole fracture system is not observable on any meaningful scale and the only realistic approach is via a stochastic model conditioned by the available data – either directly (downhole logging) or indirectly (seismic events monitored during fracture stimulation process) (Xu et al, 2010). The use of marked point processes (MPP) has proved to be an effective means of developing stochastic fracture models (Mardia et al, 2007; Dowd et al, 2007; Xu and Dowd, 2010). As more conditioning data are used, the resulting network becomes more realistic. The interactions of fractures within the network (i.e., their intersections) define pathways for the transportation of fluid, which is the key factor in assessing the performance of geothermal systems. A simple but robust and practical framework is proposed in this paper to provide a

useful tool for effective and efficient fracture intersection analyses.

Fracture Network Modelling

Fracture locations are represented by points – the centre of 2D shapes or the centroid of 3D shapes. The assessment of dispersion patterns, the density and other characteristics can be obtained by analysing a real fracture data set or a simulated fracture network. For example, the traces of fractures on an outcrop can be used to estimate the size distribution of fractures. Fracture traces on outcrops or borehole imaging can be used to help estimate fracture density.

Stochastic modelling of fractures is based on a discrete fracture network concept in which fractures are generated in a stochastic manner according to a specified underlying process. In combination with marked point processes fractures are generated as follows:

a) Fracture locations are generated based on either a Poisson (homogeneous) point process or an inhomogeneous point process.

b) Fracture orientations are derived by means of Fisher or Von-Misses distribution functions.

c) Fracture shapes (lines in 2D) are defined and fracture sizes (lengths in 2D) are drawn from its distributions, either exponential or lognormal.

d) Other features can be added as required such as aperture, transmissivity and surface roughness.

Two examples of stochastic fracture networks are shown in Figure 1 for 2D and 3D cases.

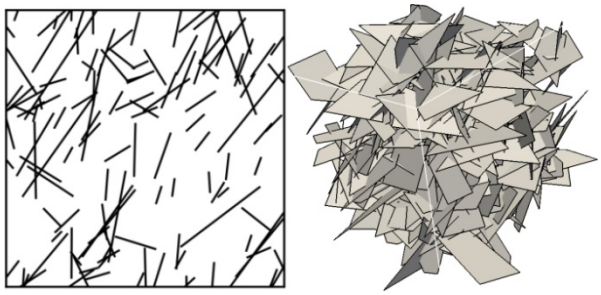

Figure 1: 2D and 3D Fracture Network Simulations via Stochastic Marked Point Processes

Other alternatives to represent fracture shapes in three-dimensional cases are ellipses (disks) or rectangles. However, polygon representation is the most general and realistic and this representation is used in our intersection analysis. We consider all fractures in this research as arbitrary shapes with varying number of nodes (vertices) and with the conditions that polygons are planar and convex. Note that every concave polygon can be reconstructed by an ensemble of convex polygons. In addition, any curved polygon (non-planar) can be divided into a set of planar polygons. Thus the framework described here (Figure 2) covers any amount of complexity of fracture shapes.

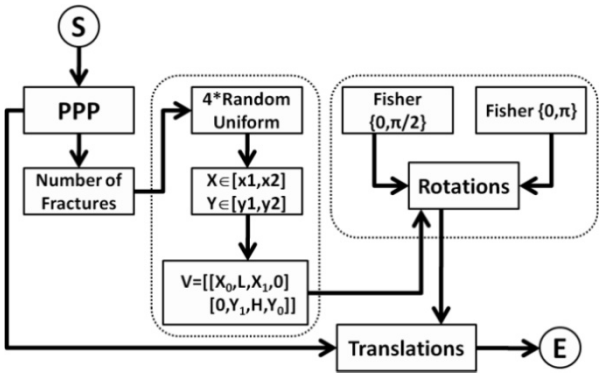

Figure 2: Framework to generate realistic fracture network by means of marked point process

Locations from Poisson point processes

An iterative process is used to generate a random number from a Poisson distribution with an intensity of λ. A uniformly distributed sequence of independent random variables is generated in the range of [0,1], $\{V_i, i=1,\ldots,n\}$. The process is stopped when one of the following conditions is satisfied (Ross 2007):

$$\prod_{i=1}^{n} V_i < e^{-\lambda} \quad \text{or} \quad \sum_{i=1}^{n} \log(V_i) < -\lambda$$

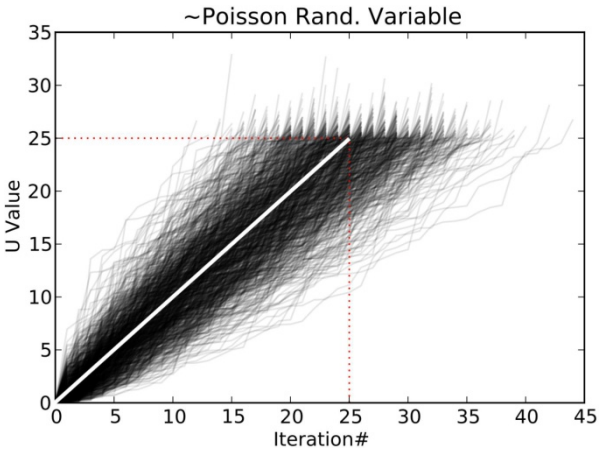

Figure 3: Demonstration of iteration number (n) for generating 1000 random number with Poisson distribution of density 25

The process is very efficient as can be seen in Figure 3 where the average number of iterations required for each random number is the density parameter (i.e., 25). Once n is determined within a region, the points are uniformly distributed within the region such as:

$$X_i\left\{(x_i,y_i,z) \in \mathbb{R}, \quad \begin{matrix} x_1 < x < x_2 \\ y_1 < y < y_2 \\ z_1 < z < z_2 \end{matrix}\right\}$$

Orientations from Fisher distribution

The orientation of a fracture plane can be described by its normal. In rock engineering, for a

fracture set, the deviation angle θ of the normal of a fracture plane from the mean normal of the set is commonly described by a Fisher distribution with parameter κ (Xu and Dowd, 2010)(Figure 4):

$$f(\theta,\kappa)=\frac{e^{\kappa\cos(\theta)}}{2\pi I_0(\kappa)},\qquad \kappa,\theta\in\mathbb{R}$$

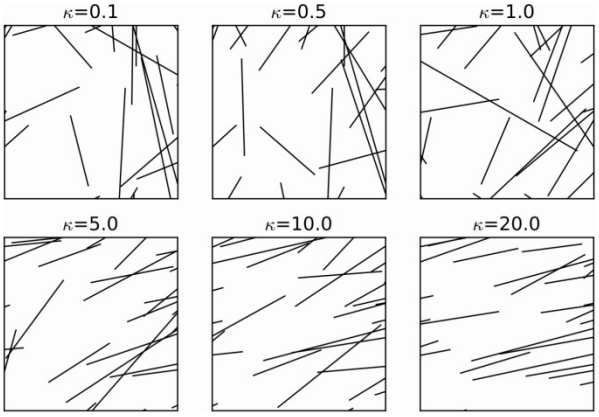

Figure 4: Demonstration of the effect of the variation of κ on Fisher function in the application for orientation angles of fractures

Any three-dimensional plane can also be described by two angles, dip and dip-direction (or azimuth), α and β:

$$\theta:\left\{\alpha,\beta\in\mathbb{R},\quad \begin{matrix}0<\alpha<2\pi\\ 0<\beta<\frac{\pi}{2}\end{matrix}\right\}$$

1- Sizes from exponential distributions

Any polygon can be bounded inside a rectangle regardless of its complexity. Therefore, to simulate the size of a fracture polygon, we first generate a rectangular shape using two numbers drawn from an exponential distribution. Then the following procedure is applied to achieve the desired polygonal shape.

Let l_1 and l_2 be two random numbers drawn from an exponential distribution defining the rectangle. Generate four points independently and randomly on the four sides of the rectangle from a uniform distribution. These four points are then connected (clockwise or counter-clockwise) to produce the final polygonal shape of the fracture. The fracture generated in this way is always convex and planar (Figure 5). Different values of l_1 and l_2 are used if anisotropy is required.

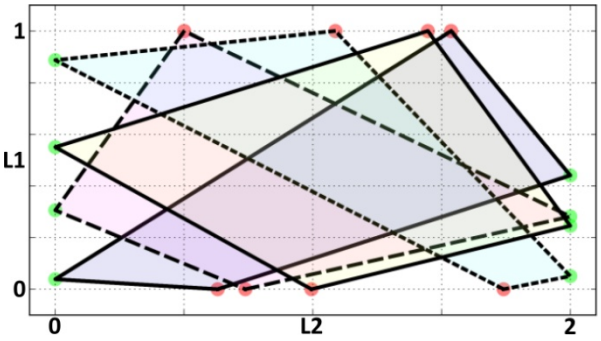

Figure 5: A robust algorithm to generate polygonal shapes for fractures

2- Rotation matrices

Based on the above definition, the transformation matrix to the local coordinate system can be written as (Vince, 2005):

$$\begin{bmatrix} cy*cz & a*cz+cx*sz & -b*cz+sx*sz\\ -cy*sz & -a*sz+cx*cz & b*sz+sx*cz\\ sy & -sx*cy & cx*cy\end{bmatrix}$$

$$cx=\cos(\phi),\qquad sx=\sin(\phi)$$
$$cy=\cos(\omega),\qquad sy=\sin(\omega)$$
$$cz=\cos(\psi),\qquad sz=\sin(\psi)$$
$$a=sx*sy,\qquad b=cx*sy$$

Where ϕ is the rotation angle around the X axis, ω is the rotation angle around the Y axis, and ψ is the rotation angle around the Z axis. Note that in practice only two rotation angles are needed so, for example, ψ can be set to zero. The rotation against the X axis in our defined coordinate system is the dip angle β (which is in the range [0, π/2]) while the rotation against the Y axis is the dip direction α and is in the range [0, 2π].

Translating the resulting polygons

To create the final fracture model, fracture polygons are first generated in the local coordinate system. The axes are then rotated so that the fractures are correctly orientated. The transformed fractures are then translated to their designated locations simulated by a point process.

Intersection Analysis (in 3D)

For the polygonal representations of fractures and the generated fracture network, there are nine possible types of intersection between any two fractures (see Figure 6).

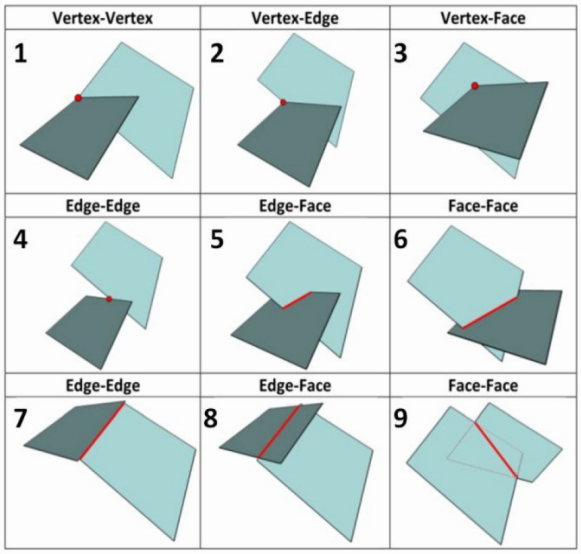

Figure 6: Possible intersection situations between two polygonal fractures in realistic fracture networks

The first four involve a vertex and the last one (Face-Face) can be seen as a special case of Edge-Edge intersection (No.7, Figure 6). The remaining four cases are of particular interest for assessing fracture intersections in a fracture network.

We propose a computationally efficient framework to analyse all intersections between fractures in a fracture network. Efficiency in this type of analysis is an important issue for large fracture networks, which is generally the case for HDR EGS. The complete framework is summarised in Figure 7.

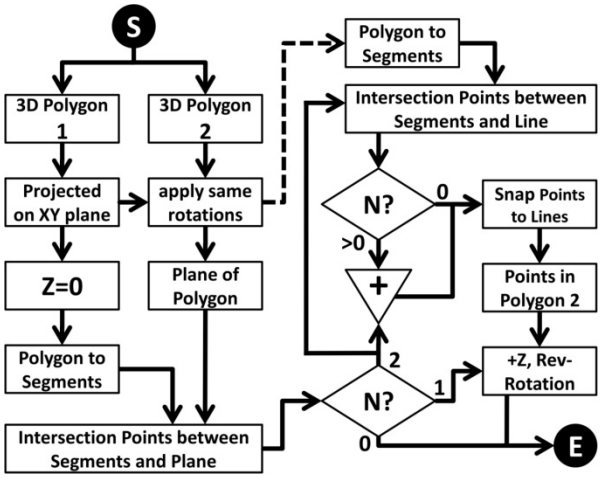

Figure 7: A full robust framework for fracture-fracture intersection analysis

Two core processes in the intersection analysis between fractures (as shown in Figure 7) are *SegXPln* (segment and plane intersection) and *SegXSeg* (segment and segment intersection). A sample pseudo-code for SegXPln is presented on Figure 8.

```
DEF SegXPln(seg, pln):
      n = pln unit normal
      u = (dx,dy,dz)[seg]
      b = (dx,dy,dz)[seg₀,pln₀]
      IF iszero(n.u) THEN
            IF iszero(n.b) THEN
                  RETURN segment is on plane
            ELSE
                  RETURN no intersection
            ENDIF
      ENDIF
      s = (n.-b)/(n.u)
      IF 0<=s<=1 THEN
            RETURN seg₀+s*u  #intersections
      ELSE
            RETURN no intersection
      ENDIF
ENDDEF
```

Figure 8: Pseudo-code for Segment-Plane intersection

The following statistics can be derived from the proposed intersection analysis.

1 - Intersection Density

One definition of fracture density in a fracture network is the density of the point process used. The density model can be parametric or non-parametric and model parameters can be estimated from sample data (Xu et al, 2003). We propose a similar definition here for fracture intersection density where points (2D applications) or lines (3D applications) of intersections are used to calculate the density value. The two are obviously related but the relationship is non-linear and complex as fracture model parameters all play a part in determining the relationship. Fracture intersections define fluid pathways and therefore are of great importance in the connectivity analysis of a fracture network model. We propose to use the density of intersection as a direct measurement of the effectiveness of the fracture network to provide pathways for fluid flow.

A 2D application example is given in Figures 9 and 10. Figure 9 shows a sample fracture network (left) and the locations of fracture centres (right: green dots) and the locations of intersection points (right: red dots). In Figure 10 it can be seen that the resulting models are different. In some areas, despite a high fracture density, the fracture intersections are limited and therefore the intersection density value is low. This part of the fracture network is expected to be less conducive for fluid flow.

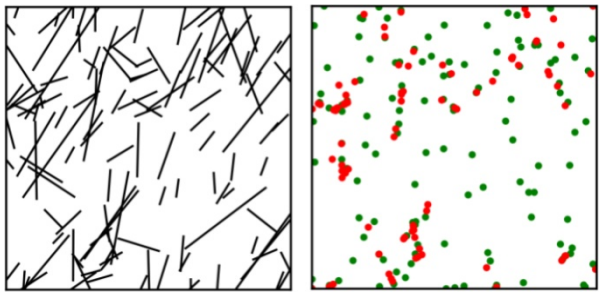

Figure 9: (left) Fracture Network HPPP; (right) Trace locations (green) and intersection points (red)

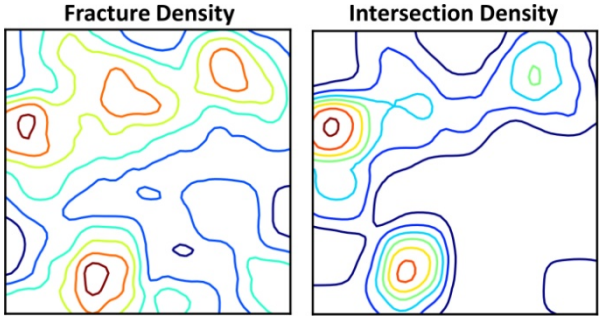

Figure 10: Density map of locations (left) and intersection points (right)

2 – Lengths of Intersection Lines

Fifteen simulations were generated to investigate the distribution of lengths of intersection lines in a three-dimensional fracture network. A homogenous marked Poisson point process was used for each realization. The histogram of the intersection lengths is shown in Figure 11 (fifteen

simulations on the same graph) with a smoothed curve fitted. It can be seen in this case that an exponential distribution satisfactorily models the distribution of lengths of intersection lines.

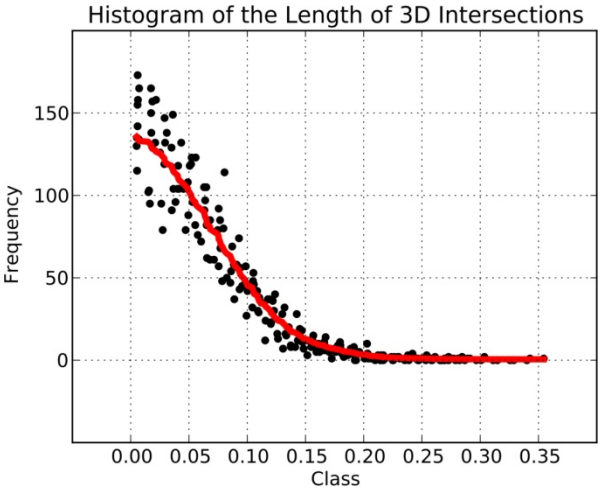

Figure 11: Distribution of the length of intersection lines in three-dimensional fracture network (class=length categories)

It is clear that long intersection lines are rare. The majority of intersection lines are of small length which demonstrates the importance of shorter intersection lines (not necessarily all from small fractures) in determining the connectivity of the fracture network.

3 - Effects of Fracture Length on Percolation State

It is interesting to investigate the relationship between percolation state and the fracture lengths of a 2D application. Fracture length is an important factor in the intersection between fractures in a fracture network and it affects the connectivity between any two points within the region.

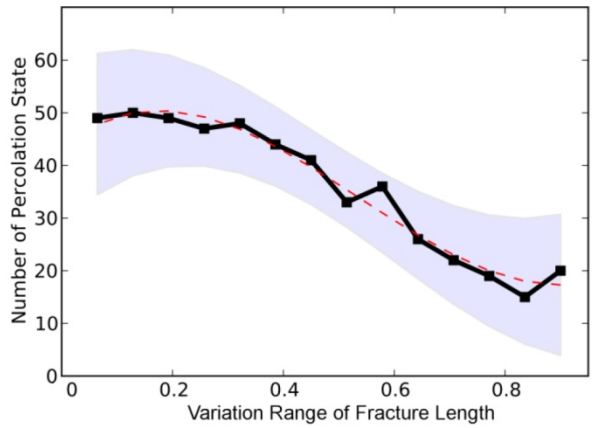

min	max	range	#state	min	max	range	#state
0.050	0.950	0.900	20	0.250	0.700	0.450	41
0.079	0.914	0.836	15	0.279	0.664	0.386	44
0.107	0.879	0.771	19	0.307	0.629	0.321	48
0.136	0.843	0.707	22	0.336	0.593	0.257	47
0.164	0.807	0.643	26	0.364	0.557	0.193	49
0.193	0.771	0.579	36	0.393	0.521	0.129	50
0.221	0.736	0.514	33	0.421	0.486	0.064	49

Figure 12: Relationship between percolation sate reached and the variation in the range of length of fractures

Figure 12 shows that larger range of variation of fracture lengths produces few number of percolation clusters for the cases investigated. In other words the homogeneity of the fracture length in the fracture network affects directly the percolation of the network. It was shown that the relationship is non-linear in this case. The simulation consists of 14 different ranges of length variations. For each variation, 50 realizations were generated. Clearly for the related analysis of connectivity evaluation of a fracture network (Xu et al, 2006) the fracture length will be a very important variable. Further study in this topic will be conducted.

Case Study - Leeds Fracture Data Set

In this section some of analyses are applied to a real fracture data set: the Leeds Fracture Data Set (Dowd et al, 2009), which was established by slicing a block of granite (Figure 13). Fractures in the data set are represented by quadratic polygons. 387 fractures are used for this study.

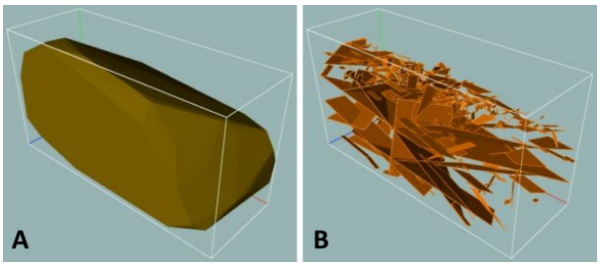

Figure 13: A 3D convex hull showing the block (left) and 387 fractures (right)

An intersection analysis of the fracture network of this block was conducted (see Figure 14) and the following results were obtained.

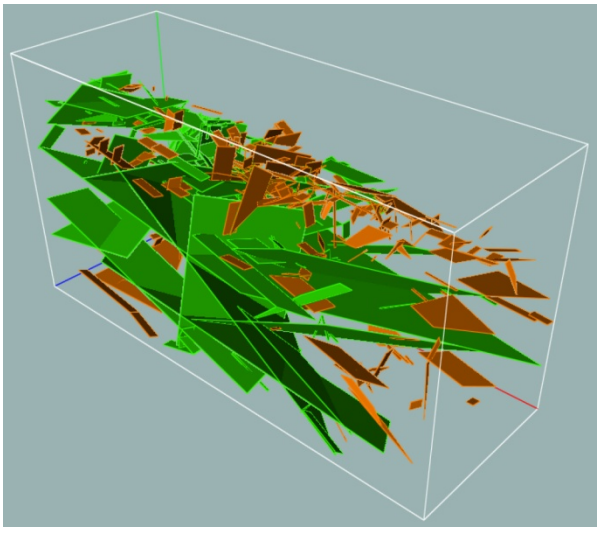

Figure 14: the result of intersection analysis which demonstrates the largest cluster of connected fractures (green)

The largest cluster (group of intersected fractures) in Figure 14 is shown in green. It can easily be seen that this cluster accounts for the percolations state of this block.

The histogram of the lengths of intersection lines for this block (Figure 15) is compatible with the results extracted from simulations (compare with Figure 11): the intersection lines have an exponential distribution.

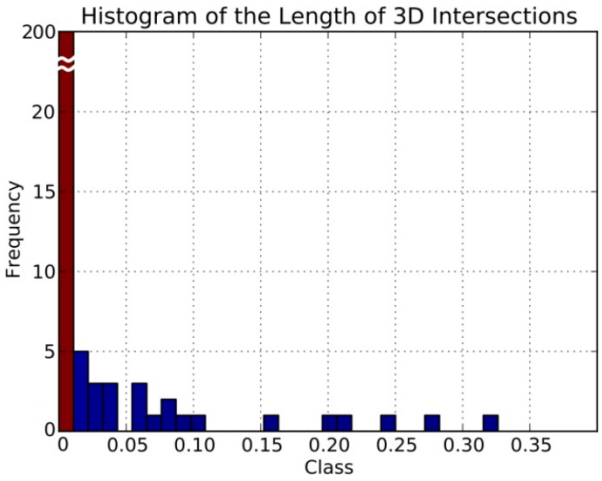

Figure 15: Distribution of the length of intersection lines in three-dimensional fracture network: Leeds Fracture Data Set (class=length categories)

The analysis of intersection density in 3D for this block is shown in Figure 16 in which subplot A is a 3D contour of the density of fracture centroid points while subplot B is the density of centres of intersection lines. It can be clearly seen that even for the same section the resulting density is different for fracture centroid points and intersection line centre points.

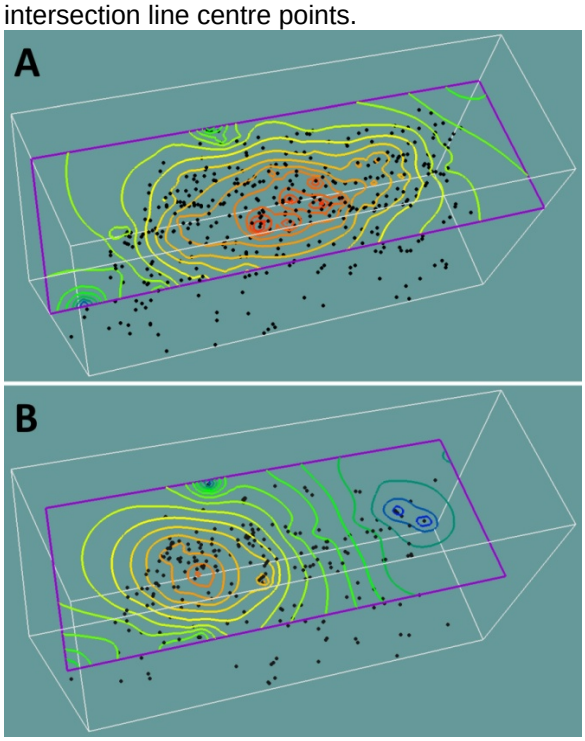

Figure 16: Density map of locations (A) and intersection points (B) of 3D fracture network, Leeds Fracture Data Set

As a result the right hand side of the block (Figure 16) has considerably less conductivity despite having a high density of fractures.

Conclusions

In this research we have developed robust algorithms/frameworks for the intersection analysis of fracture networks of any degree of complexity. Three novel analyses were conducted in this study including a) intersection density as an effective and realistic representation of the conductivity within a fracture network, b) distribution of the length of fracture intersection lines in a fracture network which is shown to be exponential, and c) the effect of length of fractures on the percolation state of a 2D fracture network. We have shown that the number of percolation clusters has a non-linear relationship to the range of variations in the fracture length. In other words, fracture size and its variability are both important variables in percolation analysis and connectivity index evaluation, which in turn are important measures for the quantification of fluid flow characteristics of fracture networks.

References

Dowd P.A, Martin J.A, Xu C, Fowell R.J, Mardia K.V, 2009, A three-dimensional fracture network data set for a block of granite, International Journal of Rock Mechanics & Mining Sciences, 46:811-818.

Dowd P.A, Xu C, Mardia K.V, Fowell R.J, 2007, A comparison of methods for the stochastic simulation of rock fractures, Mathematical Geology, 39:697-714.

Mardia K.V, Nyirongo V.B, Walder A.N, Xu C, Dowd P.A, Fowell R.J, Kent J.T, 2007, Markov Chain Monte Carlo Implementation of Rock Fracture Modelling, Mathematical Geology, 39:355-381.

MIT-led, 2010, The Future of Geothermal Energy, Technical Report, U.S. Government, http://geothermal.inel.gov, pp372.

Ross S.M, 2007, Introduction to Probability Models, Academic Press-Elsevier, USA, pp801.

Vince J, 2005, Geometry for Computer Graphics, Springer, London, p359.

Xu, C., Dowd, P. A., Mardia, K. V. and Fowell, R. J., 2006, A connectivity index for discrete fracture networks, Mathematical Geology, 38, pp. 611 – 634.

Xu C, Dowd P.A, 2010, A new computer code for discrete fracture network modelling, Computer & Geosciences, 36:292-301.

Xu C, Dowd P.A, Mardia K.V, Fowell R.J, 2003, Parametric point intensity estimation for stochastic fracture modelling, Leeds University Mining Association Journal, 16:85-93.

Xu C, Dowd P.A, Wyborn D, 2010, Optimised fracture network model for Habanero reservoir, Proceeding of Australian Geothermal Conference 2010, Australia, pp6.